J Vis (2010) 13:121–131
DOI 10.1007/s12650-009-0017-2

REGULAR PAPER

Taib Iskandar Mohamad · M. Harrison · M. Jermy · H. G. How

The structure of the high-pressure gas jet from a spark plug fuel injector for direct fuel injection

Received: 15 November 2009 / Accepted: 26 November 2009 / Published online: 8 January 2010

Abstract A spark plug fuel injector (SPFI), which is a combination of a fuel injector and a spark plug was developed with the aim to convert any gasoline port injection spark ignition engine to gaseous fuel direct injection (Mohamad in Development of a spark plug fuel injector for direct injection of methane in spark ignition engine. PhD thesis, Cranfield University, 2006). A direct fuel injector is combined with a spark plug using specially fabricated bracket connected to a fuel pipe and a fuel path running along the periphery of a spark plug body to deliver the injected fuel to the combustion chamber. The injection nozzle of SPFI is significantly bigger than normal direct fuel injector nozzles. Therefore, it is important to understand the effect of such a configuration on the injection process and subsequently the air–fuel mixing behaviour inside the combustion chamber. The flow was visualized using the planar laser-induced fluorescent technique. For safety reasons, nitrogen was used as fuel substitute. Nitrogen at 50, 60 and 80 bar pressure was seeded with acetone as a flow tracer and injected into a bomb containing pressurised nitrogen. Bomb pressure was varied to simulate the pressure inside combustion cylinder during the compression stroke where actual injections in engine experiments will take place. The shape and depth of tip penetration of the gas jet were measured. Results show that the gas jet follows the behaviour suggested by vortex ball model (Turner in Mechanics 13:356–369, 1962). The cone angle and the maximum jet width of the fully developed gas jets from the SPFI injection are 23° and 25 mm, respectively regardless of the injection pressures. The penetration lengths of the fully developed jets are between 90 and 100 mm at 8–14 ms after the start of injection, depending on the bomb and injection pressure. Jet penetration is directly proportional to the injection pressure but inversely proportional to the cylinder or bomb pressure. The penetration lengths indicate that sufficient distance should be travelled by the gas jet for satisfactory air–fuel mixing in the engine.

Keywords Air–fuel mixing · Direct fuel injection · Flow visualization · Gaseous fuel

T. I. Mohamad (✉) · H. G. How
Department of Mechanical and Material Engineering, Faculty of Engineering and Built Environment, Universiti Kebangsaan Malaysia, 43600 Bangi, Selangor, Malaysia
E-mail: taib@eng.ukm.my
Tel.: +60-3-89216967
Fax: +60-3-89259659

M. Harrison
Royal Academy of Engineering, 3 Carlton House Terrace, London SW1Y 5DG, UK

M. Jermy
Department of Mechanical Engineering, University of Canterbury, Christchurch 8140, New Zealand

1 Introduction

Natural gas is one of the most promising alternative fuels for gasoline and diesel due to its cleaner emission, lower unit price and adaptability to the operations of those engines. When an existing gasoline spark ignition engine is converted to run on compressed natural gas (CNG), a new fuel system must be installed. Gas injection in the intake manifold has been used successfully in the past, but at some loss of volumetric efficiency and accuracy in metering the fuel. Direct injection (DI) of gas into the cylinder has been implemented by drilling new holes in the cylinder head to accommodate the gas nozzles. This is expensive and time consuming. This paper deals with a system designed to facilitate fast and cost-effective conversion to CNG DI with a device which consists of a gas injection nozzle and a spark generator in one unit. This unit, called spark plug fuel injector or SPFI, simply screws into the existing spark plug hole. This paper describes a study of the fuel injection characteristics of such a system. This is important because the performance and emissions of the engines are greatly influenced by the in-cylinder flow patterns which determine many of its characteristics including air–fuel mixing, stoichiometry contour and combustion behaviour. The absence of detailed information of the flow patterns will lead the engine development to depend mainly on empiricism and intuition rather than established scientific principles. Most flow visualization of fuel injection studies deal with gas jet or liquid spray emerging from an injection nozzle or injector orifice. In this study, the gas jet from SPFI injection nozzle, which is located at some distance from injector orifice, was investigated. The injection nozzle of an SPFI is significantly bigger than those of conventional fuel injectors and the injection penetrates into a high-pressure turbulent gas in the engine cylinder.

The objective of this study is to investigate the shape, development and depth of penetration of gas jets from the SPFI. A laser diagnostic method was used to visualize the gas jet developed in the bomb. Because compressed nitrogen is injected into nitrogen, the imaging method must be able to differentiate the injection and surrounding gas when injection takes place. The planar laser-induced fluorescent (PLIF) technique was chosen. With this technique, the tracer must be able to produce a visible effect when excited by the laser sheet, and must remain in the appropriate phase and the signal should remain proportional to tracer concentration.

The applications of LIF method in methane-fuelled engines are mainly found in flame and emission studies. A quantitative study on temperature, OH, and CH_2O effects on the stabilization of lifted turbulent methane flames issuing into a high temperature vitiated co-flow was carried out using LIF method (Gordon et al. 2008). Quantitative measurements of NO concentration along the centerline of atmospheric pressure, methane–air, counter-flow partially premixed flames using the laser-induced fluorescence technique have also been carried out (Ravikrishna and Laurendeau 2000). A study on micro-jets in a turbulent confined cross flow using PLIF was carried out to investigate the concentration of methane in the mixing region of the flow (Kelman et al. 2006). A number of tracer materials have been used in PLIF imaging including acetone, pentanone-3, NO_2 (Hayashida et al. 1999), and rhodamine (Yamakawa et al 2001). Hirasawa et al. (2007) investigated the possibility of various LIF tracers, namely, acetone, methylethylketone, acetaldehyde ethylbenzene, anisole, aniline, and naphthalene to measure the temperature profiles in a two-dimensional gas flows based on two-colour fluorescence induced by a one-colour laser. Acetone was chosen to be the LIF gas tracer in this experiment as it has been successfully utilised in gaseous flow measurement as reported by a number of sources (Lozano et al. 1992; Choi et al. 2002; Olsen and Willson 2002). Further studies on SPFI regarding these aspects will be carried out in the future. All these PLIF-related studies are focused on flame and emission analysis, liquid fuel injection and injection process of a gas into another gas. Limited studies were done on the injection and environment of the same gas. This paper will discuss the success of imaging and qualitative analysis of single-species gas-to-gas injection using LIF technique for analysing the SPFI. The results will be used for improving the design of this novel product.

2 Spark plug fuel injector

The SPFI is a device developed to convert any port injection engine to direct injection gaseous fuels (natural gas, hydrogen, etc.). Normally, converting to direct injection requires modifications to or replacement of the cylinder head to accommodate extra holes for fuel injectors and possibly modifying the piston crowns which incur a high cost. With SPFI, this cost can be reduced because no modification on the original engine structure is required. It is a technically simpler conversion system by only replacing the existing spark plug

with SPFI. As a result, users will not only benefit from an alternative low cost conversion, but also can enhance the engine performance compared to currently available conversion system with port fuel injection. In addition, SPFI also can be utilised for dual-fuel systems such as gasoline-CNG, gasoline-hydrogen and CNG-hydrogen. Figure 1 shows the SPFI and associated components. The technical drawings and connection to an Audi-FSI direct gasoline injector (DGI) encapsulated in a bracket are shown in Fig. 2. The SPFI consists of a spark plug with a 1 by 2 mm square cross-section fuel path cut out along the periphery of its threaded section and a steel tube soldered to the end of the cut section. A DGI is connected to it using a specially developed bracket to the end of the fuel path. The distance from the DGI injection nozzle to the SPFI nozzle is 11 cm. The DGI injector is connected to a 230 bar methane bottle through a pressure regulator where methane pressure is reduced to the desired pressure. A specially developed injection control was used to regulate fuel injection by referencing crank angle signals from a camshaft encoder. The length of injection pulse determines fuel mass delivered, therefore air/fuel ratio to the cylinder.

3 Experimental methods and procedures

3.1 Injection chamber and LIF imaging

The experimental setup can be categorised into four groups; (1) a laser-optical lens system, (2) an imaging system, (3) a fuel supply system and, (4) a fuel chamber equipped with windows in which the fuel substitute is injected (termed the "bomb"). The details of the experimental setup are shown schematically in Fig. 3. The fuel injection driver circuit was synchronised with the camera and laser systems. A MOSFET transistor, acting as a gate/bridge between a power supply unit and the SPFI, is excited by the output of a pulse generator which functioned as the main driver to the experiment. At the same time, the pulse generator output was connected to another pulse/delay generator where its signal was sent to the laser source. The laser source simultaneously sent a signal to the camera so that the laser pulse was synchronised with the opening of the shutter. An oscilloscope was connected to both pulse/delay generator to measure the delay between initiation of fuel injection and image capture. For every 0.5–1.0 ms interval (delay with respect to

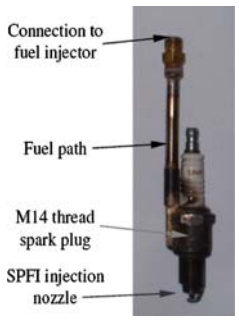

Fig. 1 Spark plug fuel injector

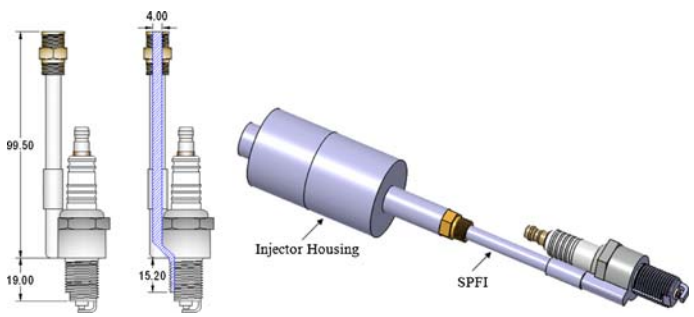

Fig. 2 *Left* Technical drawing of SPFI (units in mm) and *right* SPFI connected to injector housing

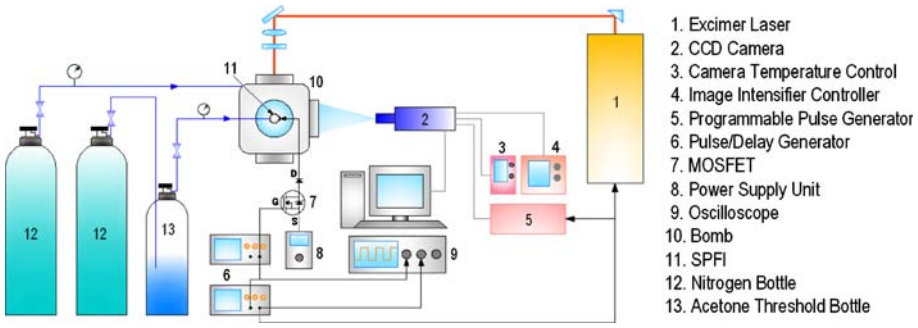

Fig. 3 Schematic of the PLIF imaging of SPFI injection

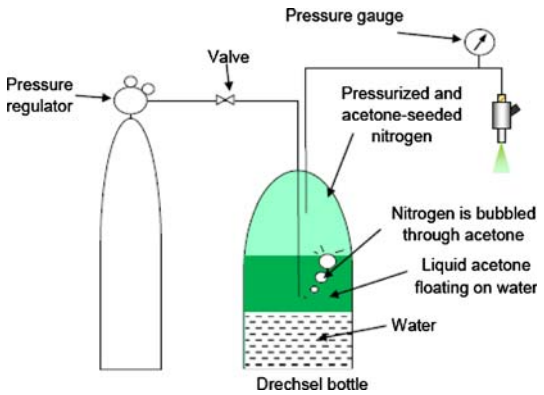

Fig. 4 Nitrogen acetone doping mechanisms (Drechsel bottle) for SPFI spray imaging

injection signal), 20 images were captured; therefore, the sequence of jet development images was independent of the laser frequency.

The plume of fuel emerging from the injector nozzle was imaged. The plume was illuminated with a 100 mm high, 0.5 mm thick light sheet from a Lambda-Physik XeCl excimer laser (308 nm) with 100–200 mJ/pulse and was imaged with a LaVision SprayMaster 3 camera with image intensifier and 105 mm Nikkor UV lens. Laser-induced fluorescence (LIF) images were taken of fluorescence emitted by the acetone mixed with nitrogen. The LIF is emitted by both droplets and vapour and the signal is proportional to the local mass concentration. Images were taken at several different times after the start of the injector current pulse. At each time, 20 images were taken from successive cycles. The camera settings were f/8, intensifier gate 200 ns, intensifier gain $\times 60$, camera gain $\times 95$. The images were corrected for background intensity and light sheet intensity variations with LaVision DaVis 6.2 software.

The nitrogen acetone doping mechanism (Drechsel bottle) is shown in Fig. 4. The nitrogen is bubbled through the acetone and trapped in the upper part of the threshold bottle. The trapped gas increases its pressure and as it reaches the desired injection pressures, the supply valve is closed. An outlet gas pipe is attached to the bottle, positioned above the surface of acetone, thus only acetone-saturated gas is delivered to the SPFI. The amount of seeded acetone is determined based on the saturated vapour pressure of acetone at the room conditions which equals the partial pressure of acetone in the seeded gas. Acetone concentration was kept constant by adjusting the injection frequency to give sufficient time for building up acetone concentration for the next injection. The supply gas and bomb were maintained at room temperature using a water bath. The evaporative cooling in the acetone bottle was kept to a minimum during all pulse durations. The pressure gauge on the gas pipe near SPFI was used to determine the injection pressures.

The experiments were carried out by referencing the motorised cylinder pressure of a single cylinder Ricardo E6 engine (Mohamad 2006). Figure 5 shows the non-firing cylinder pressure during the compression stroke and the injection timings for stoichiometric air–fuel ratio operations. For 80 bar injection pressure, the optimal injection time is at 215° BTDC of compression stroke (Mohamad 2006). For 50 and 60 bar injections, the optimal injections were at 170° BTDC. Fuel injection durations were 6, 10 and 12 ms for 80, 60 and 50 bar injection pressures, respectively in order to supply a stoichiometric quantity of fuel. At

1,100 rpm, these injections cover 40, 66 and 79°CA, respectively as shown in Fig. 6. Taking into account the fuel delivery delay due to the lengthy fuel path in the SPFI, it was decided to perform injections at three bomb pressures: 1, 3 and 10 bar. The 1 and 3 bar pressure represent the range of actual injection cylinder pressure, while the 10 bar pressure was chosen to investigate the effect of gas jet if injection is delayed at later stage of compression stroke.

3.2 Image calibration

It is important to quantify the injection penetration and the width of the gas plume from the images. The bomb viewing window allows 110 mm circular diameter visual access to the injection gas flow. Calibration of gas jet dimensions was achieved by imaging a known scale object attached to the fuel injection vertical plane as shown in Fig. 6. Figure 7 shows a calibration image captured by the CCD camera and compared with a PLIF image with no gas injection. The bright spots at the top of the PLIF image are due to strong elastic scattering of the laser light from the injector and holder breaking through the PLIF filter. The speckled pattern in the bulk of the image is due to thermal and cosmic ray noise in the intensifier and CCD. High intensifier voltage and low level of signal leads to low signal-to-noise ratio. Much effort was applied to avoiding this background noise and improvements were made. In addition, the design of the doping system was limited by a need to operate it at high pressures (up to 80 bar) and limited supply of acetone (hence the immersion of the nitrogen supply tube was limited).

4 Results and discussion

Images of gas jets from SPFI nozzle were obtained successfully with the PLIF method. The images shown in Figs. 9, 10, 11 are the consecutive images of gas jet at various injection and bomb pressures. The bright white areas penetrating from the top of each image indicates the injected gas presence. The intensities of brightness can be used to describe qualitatively the gas concentration. It is important to note that because the acetone-doped nitrogen remains static in the injection fuel line due to the slow rate of injection in this

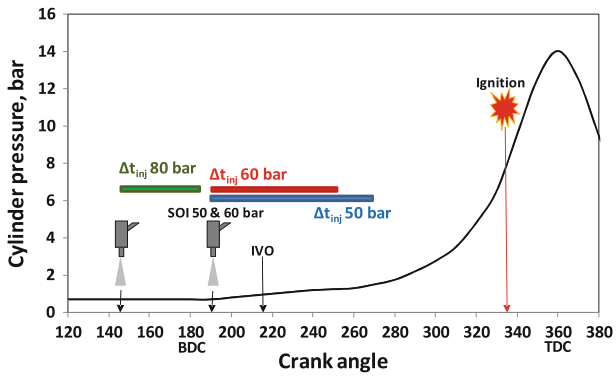

Fig. 5 Cylinder pressure of motorised Ricardo E6 engine ($r = 10.5$, $N = 1{,}100$ rpm), starts of injections and injection timings (Δt_{inj}) derived from engine experiments

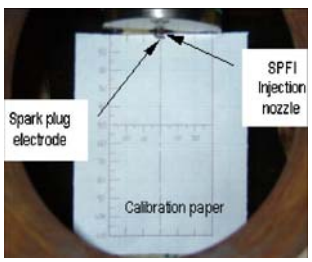

Fig. 6 Calibration of fuel injection measurement

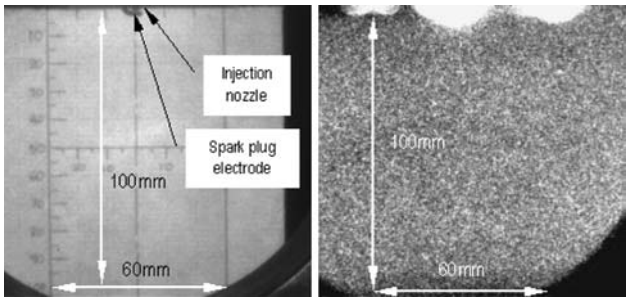

Fig. 7 Calibration image (*left*) and PLIF image with no gas injection (*right*)

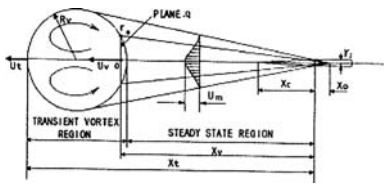

Fig. 8 The vortex ball model (Turner 1962; Boyan and Furuyama 1998)

experiment (once in every 1 s), it was possible that some of the acetone settled or condensed to the pipe walls, thus reducing the concentration of doping. Nevertheless, the jets are clearly seen in the figures. The shapes of the gas jets are in good agreement with the vortex ball model (Turner 1962; Boyan and Furuyama 1998). Figure 8 shows the vortex ball model which is a theoretical model that assumes the gas transient jet can be characterized as a spherical vortex interacting with a steady-state jet.

The injection durations for 50, 60 and 80 bar fuel pressures on the Ricardo E6 engine were 12, 10 and 6 ms, respectively. These values correspond to the stoichiometric fraction of methane for the engine tests. A fully developed gas jet refers to the gas plume with longest jet tip penetration before detachment from the SPFI nozzle. In general, it can be seen that the fully developed gas jets from the SPFI injection were relatively narrow, with about 23° cone angle and 25 mm of maximum width in a fully developed gas jet as shown in Figs. 9, 10, 11. The cone angle is specified by measuring the angle generated by a triangle connecting the centre of SPFI nozzle and the widest horizontal span of the gas jet as shown in Fig. 12. The jet tip penetration length and jet width were defined based on the lowest acetone concentration detectable. Figure 12 shows the visual definition of the tip penetration length and jet width. However, it is important to note that the actual values of width and penetration length measured depend on the threshold of sensitivity of the PLIF system. The penetration length of the fully developed gas jet is between 90 and 100 mm at 8–14 ms after the SOI.

The results show that at all injection pressures, the first appearance of gas jet can be seen at 2.5 ms after SOI which coincides with the first interval of imaging. However, the images at this interval were not shown in Figs. 9, 10, 11. It is believed that if the interval is decreased, the first appearance of gas jet can be well defined with respect to different injection pressures. The fully developed jets (green squares background) appear at different times. Higher injection pressure results in faster development of a fully developed jet which is defined by the furthest distance of jet tip penetration, while the plumes were still attached to the injection nozzle. In addition, increasing injection pressure reduces the effective fuel delivery time which is measured from the SOI signal to the time of gas plume detachment from the injection nozzle. Bomb pressure affects the magnitude of tip penetration and effective fuel delivery time. Increasing bomb pressure leads to shorter jet penetration and slower effective delivery time.

Figure 12 shows the fully developed gas jets from a 60 bar injection pressure into 3 bar bomb pressure. A significant amount of background scattering on the image can be seen. The scattering was believed to be the result of minor illumination of the background gas in the bomb by the laser sheet. It was made worse by the need to pick out slight fluorescence from a lightly doped injection gas. This however, did not prevent the visualization of gas jet development and qualitative determination of gas jet parameters. The penetrations of gas jet based on the PLIF imaging experiments are shown in Fig. 13. Figure 14 shows the effect of injection and bomb pressure on tip penetration. Jet penetration is proportional to square root of injection time, except

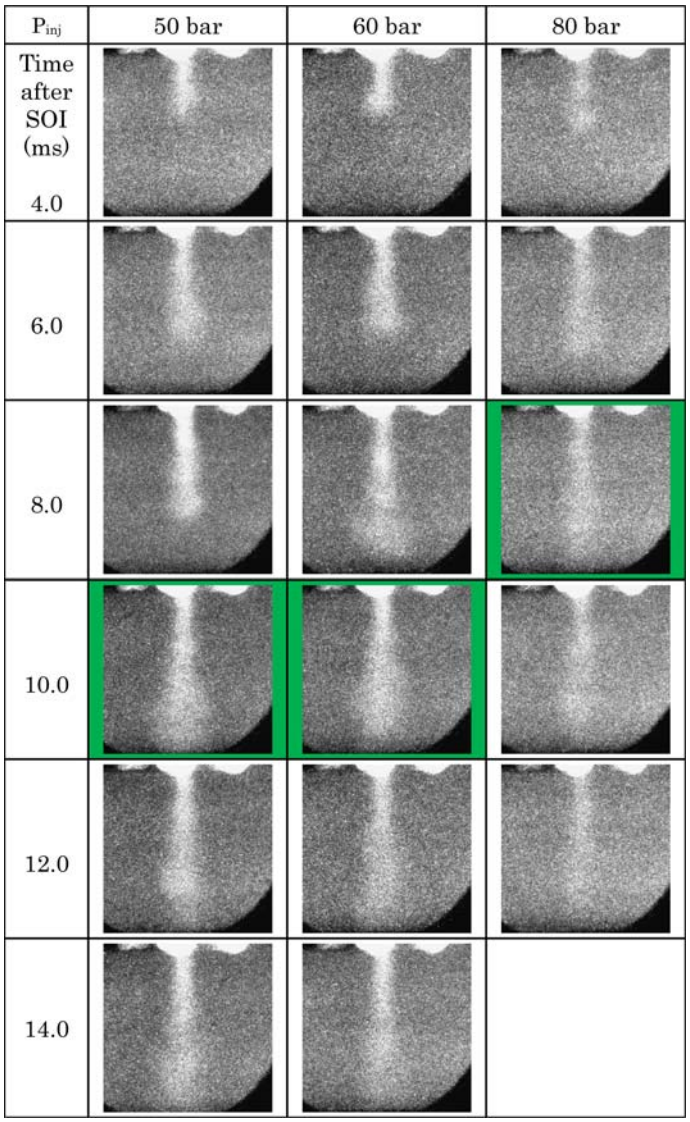

Fig. 9 Consecutive images of various injection pressures at 1 bar bomb pressures. Fully developed gas plume are indicated by the *green square backgrounds*

in the early phase. As the bomb pressure increases, jet penetration reduces. However, for the same bomb pressure, the variation in penetration lengths with changing fuel pressure is relatively small due to SPFI injection nozzle exit flow were at sonic conditions for all injection pressures. Sonic conditions result in choked flow; therefore, gas velocity remains constant except when flow temperature increases. However, the mass flow rate at the sonic conditions not only depends on flow temperature, but also depends on the density of the injected gas which is proportional to supply pressure. Therefore, mass flow rate determines the length of injection duration and in certain degree affected the length of jet penetration. As shown in Figs. 9, 10, 11, at 8 ms, with 3 bar bomb pressure where gas jets were near fully developed, the penetration lengths are highest at 80 bar and lowest at 60 bar injection. The jet from 60 bar injection is slightly wider but shorter than the one from 50 bar injection.

Measurement of jet tip penetration was performed from 15 images of each injection condition. Error analysis was done with respect to the measured data. Table 1 shows the error analysis of jet tip penetration measurements. The values are tabulated because the errors are too small to be shown in Figs. 13 and 14. The average error was ± 0.30 mm and the highest error was found to be at ± 0.48 mm or 3.9% of the measured data. These errors were sourced from a number of factors. Variation of acetone temperature affects the concentration of acetone in the compressed nitrogen. Assuming laser power and camera sensitivity remain

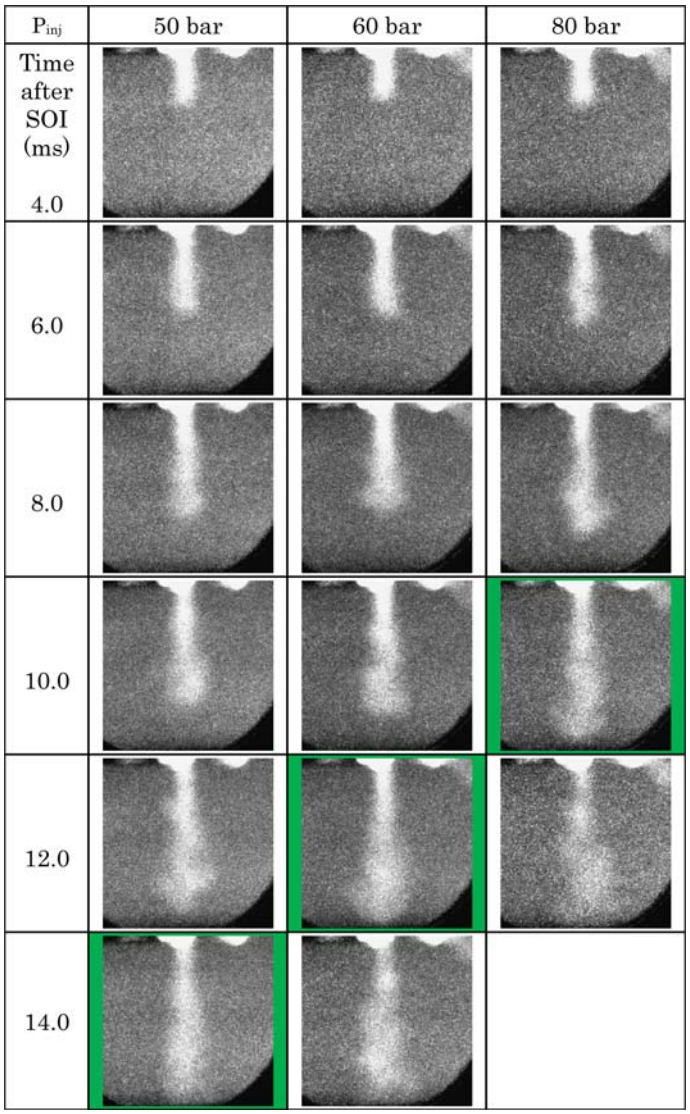

Fig. 10 Consecutive images of various injection pressures at 3 bar bomb pressures. Fully developed gas plume are indicated by the *green square backgrounds*

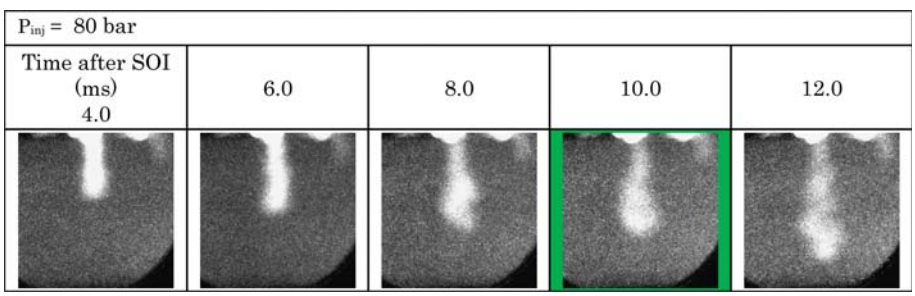

Fig. 11 Consecutive images of 80 bar injection pressures at 10 bar bomb pressure. Fully developed gas plume are indicated by the *green square backgrounds*

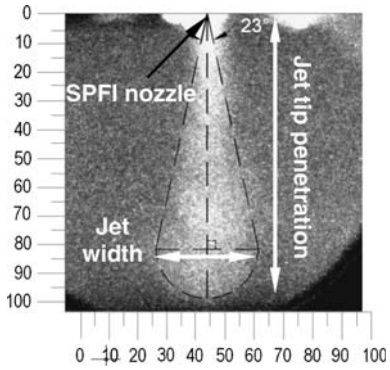

Fig. 12 Fully developed gas jet from SPFI at 60 bar injection and 3 bar bomb pressure

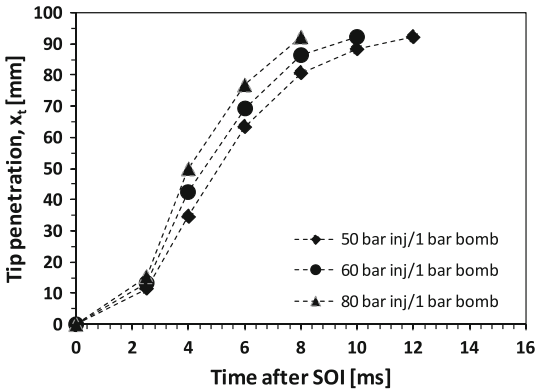

Fig. 13 Effects of injection pressure on the SPFI jet tip penetration

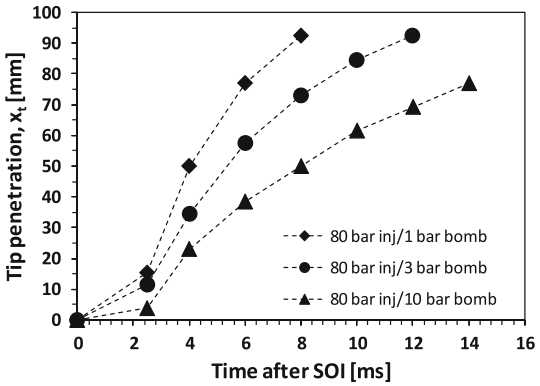

Fig. 14 Effect of bomb pressure on the SPFI jet tip penetration

constant, the variation of acetone concentration means variation in location of threshold of fluorescent signal. Visual error while measuring the jet parameters from the images was another source. However, the error was proven to be relatively low.

Figure 15 shows the projected fully developed gas jet at 60 bar injection pressure and 1 bar bomb pressure inside the combustion chamber with piston at BDC where the engine experiments were carried out. It indicates the sufficient jet penetration length especially during the later part of compression stroke. However, the width of the jet and the direction of injection away from the point of ignition could be detrimental to the engine performance. SPFI utilises a fuel injector (Audi-FSI direct injector) which is optimised for direct injection and stratified charge operations. However, the optimization of nozzle design and orientation to give best effect on stratified charge direct injection has not been taken advantage of by the

Table 1 Error analysis of jet penetration measurements

P_{inj} (bar)	50		50		60		60		80		80		80	
P_{bomb} (bar)	1		3		1		3		1		3		10	
Time (ms)	X_t mm	Error ±	X_t mm	Error ±	X_t mm	Error ±	X_t mm	Error ±	X_t mm	Error ±	X_t mm	Error ±	X_t mm	Error ±
0	0.0	0.00	0.0	0.00	0.0	0.00	0.0	0.00	0.0	0.00	0.0	0.00	0.0	0.00
2.5	11.5	0.31	7.8	0.28	12.4	0.48	9.6	0.26	15.4	0.36	11.7	0.28	4.1	0.25
4	35.0	0.27	30.9	0.28	42.7	0.27	32.7	0.26	50.4	0.32	35.4	0.30	23.2	0.28
6	62.9	0.28	50.0	0.36	69.1	0.34	53.7	0.34	77.2	0.36	57.7	0.26	38.7	0.36
8	81.2	0.27	63.2	0.36	86.2	0.37	69.2	0.26	92.3	0.26	73.1	0.26	50.4	0.32
10	88.8	0.27	73.2	0.28	92.4	0.28	78.8	0.26			84.6	0.26	61.7	0.28
12	92.3	0.31	80.9	0.28			86.3	0.25			92.4	0.42	69.5	0.25
14			88.7	0.31			92.2	0.28					77.2	0.36
16			91.9	0.32										

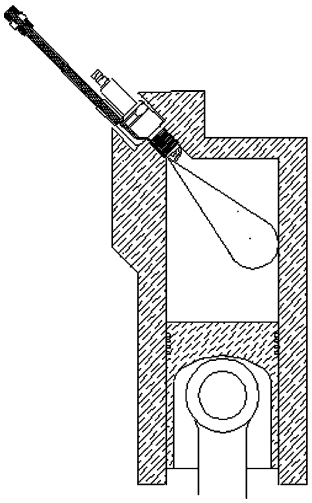

Fig. 15 A fully developed gas jet inside the combustion chamber with piston at BDC

SPFI system yet. As a result, the effective fuel injection behaviour is determined mainly by the injection nozzle as well as the fuel path. This work has given a qualitative understanding of the injection and mixing behaviour which is useful for design optimization process of SPFI.

5 Conclusion

Visualization of gas jet development from a spark plug fuel injector has been successfully implemented using planar laser-induced fluorescence with acetone as the flow tracer. Imaging a gas jet in a gas environment, which has been difficult to achieve previously, is now a reality. The gas jet agrees with the vortex ball model (Turner 1962; Boyan and Furuyama 1998). The jet is generally narrow with around 23° cone angle and 25 mm of maximum width in a fully developed gas jet. The penetration length of the fully developed gas jet is between 90 and 100 mm at 8–12 ms after the SOI depending on the injection and bomb pressure. Penetration length is proportional to square root of time, except in the early phase of jet development. In addition, jet penetration is directly proportional to the injection pressure but inversely proportional to the bomb pressure.

References

Boyan X, Furuyama M (1998) Jet characteristics of CNG injector with MPI system. JSAE Rev 19:229–234
Choi HJ et al (2002) Visualization of concentration field in a vortex ring using acetone PLIF. J Vis 5–2:145–152

Gordon RL et al (2008) Simultaneous Rayleigh temperature, OH- and CH_2O-LIF imaging of methane jets in a vitiated co-flow. Combust Flame 155(1-2):181–195
Hayashida M et al (1999) Investigation of performance and fuel distribution of a direct injection gas engine using LIF measurement. SAE 1999-01-3291
Hirasawa T, Kaneba T, Kamata Y, Muraoka K, Nakamura Y (2007) Temperature dependence of intensities of laser-induced fluorescences of ethylbenzene and naphthalene seeded in gas flow at atmospheric pressure: implications for quantitative visualization of gas temperature. J Vis 10–2:197–206
Kelman J et al (2006) Micro-jets in confined turbulent cross flow. Exp Therm Fluid Sci 30–4:297–305
Lozano AB et al (1992) Acetone: a tracer for concentration measurements in gaseous flows by planar laser-induced fluorescence. Exp Fluids 13–6:369–376
Mohamad TI (2006) Development of a spark plug fuel injector for direct injection of methane in spark ignition engine. PhD thesis, Cranfield University
Olsen DB, Willson BD (2002) The impact of cylinder pressure on fuel jet penetration and mixing. ICE 39:233–239
Ravikrishna RV, Laurendeau NM (2000) Laser-induced fluorescence measurements and modeling of nitric oxide in counterflow partially premixed flames. Combust Flame 122–124:474–482
Turner JS (1962) The starting plume in neutral surroundings. J Fluid Mech 13:356–369
Yamakawa MS et al (2001) Measurement of ambient air motion of D.I. gasoline spray by LIF-PIV. In: The proceedings of the fifth international symposium on diagnostics and modeling of combustion in internal combustion engines (COMODIA 2001), Nagoya, Japan